Tetrahedron Vol 36, pp 3209 to 3217

0040-4020/80/1115-3209/$02.00/0

ELECTRONIC STRUCTURE AND REACTIVITY OF PROPELLANES†

THE STEREOCHEMISTRY OF DIELS–ALDER- AND RELATED CYCLOADDITIONS IN THE SERIES OF [4.4.2] AND [4.4.3] PROPELLANES; MODELS AND INTERPRETATIONS

MICHAEL C. BÖHM

Institut für Organische Chemie der Technischen Hochschule Darmstadt, D-6100 Darmstadt, West Germany

and

ROLF G. EITER*

Organisch-Chemisches Institut der Universität Heidelberg, D-6900 Heidelberg, West Germany

(*Received in Germany* 13 *November* 1979)

Abstract—The stereochemistry of the products obtained by Diels–Alder addition of **1** to **2–6** and **14** and **15** has been rationalised. In case of the propellanes **2–6** a frontier MO approach substantiated by extended Hückel calculations has been invoked. For **14** and **15** the Coulomb interaction between the polar SO and SO_2 groups and the dienophile is decisive for the observed stereochemistry.

The stereochemistry of cycloaddition reactions in the series of polyenic propellanes has been developed in recent years.[1–3] Of special interest are the [4.4.3] and [4.4.2]propellanes belonging to the point group C_{2v} (two examples are shown below) where the substituents in the [3] or [2] bridge show a highly directing effect in cycloaddition reactions.

Certain functional groups favour the formation of a *syn* product, while others lead to a preponderance of the *anti* product (for the definition of *syn* and *anti* see below). To get some insight into the factors determining the directing effect we will develop in this paper some model concepts which allow an interpretation of the different reaction patterns

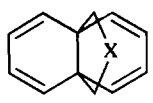

[4.4.3]propellane

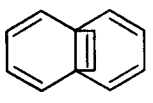

[4.4.2]propellane

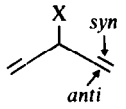

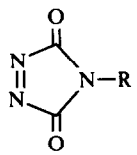

1

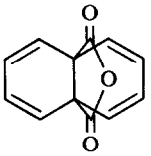

2

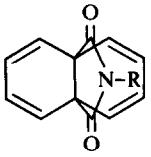

3

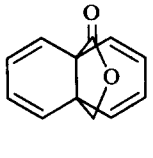

4

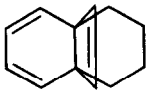

5

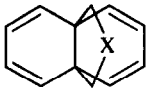

6

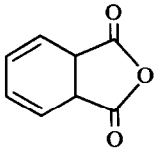

7

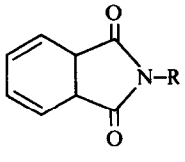

8

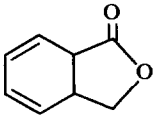

9

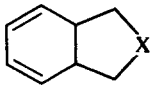

10

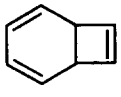

11

X = O, S, N R
R = aklyl, aryl

†Dedicated to Prof. Dr. D. Ginsburg on the occasion of his 60th birthday.

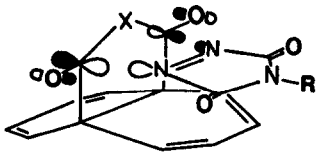

Fig. 1. Schematical drawing of the antisymmetric linear combination n_- and π^*_- of **1** and **2** or **3** respectively.

encountered in this class of compounds which can be extended to similar systems.

In the first part we will discuss the outcome of the Diels–Alder cycloaddition between the dienophile, 1,2,4-triazoline-3,5-dione (**1**) and the propellanes **2**–**6**.[1–4]

Within this series of propellanes the compounds **2** and **3** as well as the bicyclic compounds **7** and **8** favour the formation of the *syn*-Diels–Alder adduct. On the other hand, the corresponding *anti*-adduct is obtained when the reaction takes place between **1** and the propellanes **5**, **6**, **10** and **11**.[1–4] Compounds **4** and **9** give a mixture of *syn* and *anti*-adducts.

Based on qualitative arguments of perturbation theory[5] we explained the *syn* directing effect in the corresponding propellanes as due to a secondary orbital interaction between the n_- lone-pair combination of **1** and the antisymmetric π^*_{CO} molecular orbital of the CO–X–CO fragment.[3,4,6,7] This is shown schematically in Fig. 1. This secondary orbital effect lowers the activation energy of the *syn* transition state. For the *anti* transition state no such stabilization is possible.

By means of the Extended Hückel (EH) method[8] we have calculated the potential surfaces for *syn* and *anti* attack for the cycloaddition between **1** (R–H) and **7**. We have assumed that the plane of symmetry is conserved during the whole reaction. For a two dimensional map we varied the **Oa** vector for the dienophile **1** with respect to the π-unit of **7** and calculated the total energy E_{z+} for one point of the hypersurface with a definite $+z$ coordinate and the total energy E_{z-} for the corresponding $-z$ coordinate (see Fig. 2).

The difference $\Delta E = E_{z+} - E_{z-}$ between the energy values is plotted in Fig. 2 as a function of y and |z|. This construction (energy difference between $+z$ and $-z$ geometry) allows us a separation into the secondary orbital interaction in which we are interested and into the energetical changes which are due to the Diels–Alder cycloaddition. This latter aspect has been discussed in recent years in a series of publications dealing with the mechanism and the transition state of a variety of Diels–Alder reactions.[9–12] While MINDO/3 predicts a "one bond" biradicaloid transition state[9] as a result of closing the bonds stepwise, *ab initio* calculations[10–12] postulate a synchronous product formation via a transition state of C_s symmetry.[13,14]

Inspection of the map displayed in Fig. 2 clearly shows two different regions for *syn*-attack, leading to stabilization or destabilization for the assumed symmetrical transition state. Above the dienic moiety the calculations predict a region where the formation of the *syn*-product is unfavoured due to an antibonding secondary orbital interaction between the n_+ lone-pair combination of **1** and the lone-pair of the central oxygen atom of **7**. If this antibonding interaction were to dominate, anti-attack should be favoured.

Besides the antibonding sphere there is, however, an area which stabilizes the formation of the *syn* adduct because the destabilizing interaction just mentioned is overcompensated by a bonding interaction between π^*_{CO} of **7** and n_- of **1** as indicated in Fig. 3. If we now compare the profile of the energy map in Fig. 2 with calculated transition state geometries of Diels–Alder reactions[9–11] (the predicted C...C bond lengths are 2.2 Å) we realize that the formation of the new σ bonds

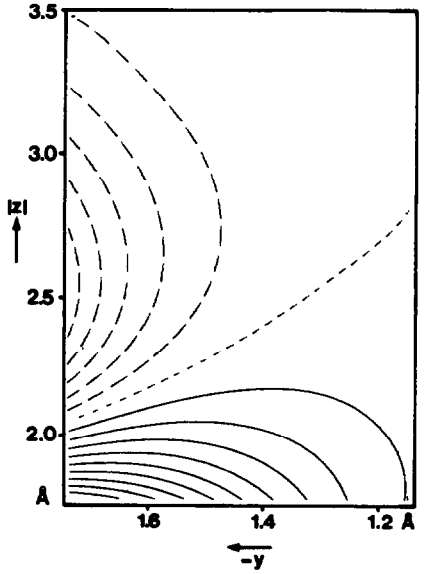

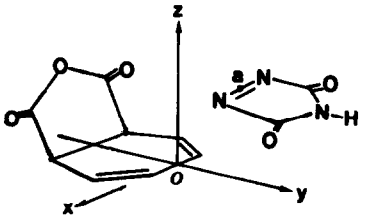

Fig. 2. Contour diagram of the EH potential surface for the addition of **1**–**7**. The contours are drawn every 4 kcal/mol and represent the difference in energy between addition *syn*(+z) and *anti*(−z) relative to the anhydride group. The full lines correspond to situations where *syn*-addition is energetically favoured, the broken lines indicate *anti*-addition.

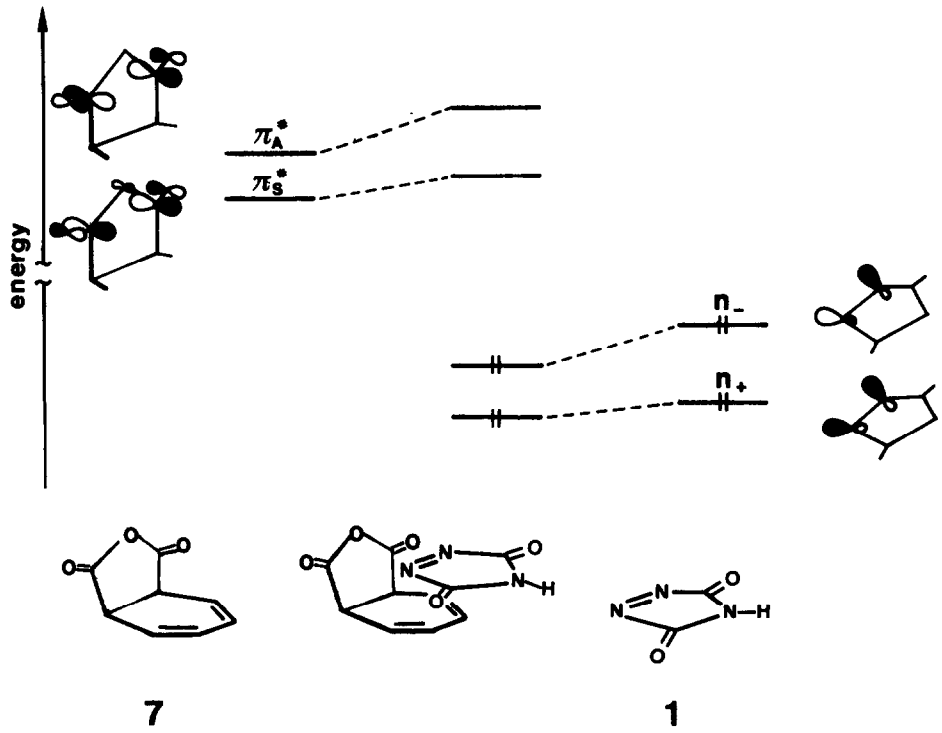

Fig. 3. Qualitative interaction diagram for the *syn*-approach of 1–7. Only the interactions between the lone-pairs on the nitrogen atoms of 1 and π carbonyl orbitals are shown. The interaction between the π orbitals of the carbonyl group and the n orbitals of 1 is omitted.

takes place in a region where *syn*-attack is favoured considerably by secondary orbital interaction.

According to our model calculation the secondary orbital effect lowers the activation energy by 4–6 kcal/mol. This lowering of the energy has to be compared with the calculated activation energy for the reaction *cis*-butadiene + ethylene which amounts from 20 to 40 kcal/mol[7–9] and the experimentally determined value for this reaction which is 27.50 kcal/mol.[15]

The stabilization of the *syn*-transition state by a secondary orbital effect is most efficient if the cycloaddition between **1** and **7** occurs via a transition state of C_s symmetry as indicated schematically in Fig. 4(a).

In case of an unsymmetrical transition state like the one indicated in Fig. 4(b) the stabilization via a secondary orbital effect is less efficient. This has been verified experimentally in case of the monocarbonyl compounds **4** and **9**. In these examples a large amount of *anti* product is formed in addition to the *syn* product.

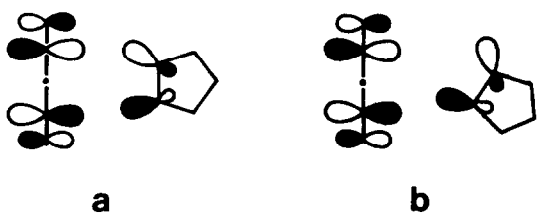

Fig. 4. The linear combinations $\pi^{\pm}$ and n_ in case of a concerted (a) Diels–Alder addition and for a non concerted (b) case.

At first sight one might expect that Diels–Alder reaction between **1** and **5** or **11** should also occur preferentially from the *syn* side. The rationale for this expectation might be the bonding interaction between the π^* orbital of the ethylene bridge on the n_ lone-pair combination of **1** which is shown schematically in Fig. 5. Inspection of the available experimental data, however, clearly indicates that **1** adds to **5** and **11** preferentially from the *anti* side.

An analogous investigation of the potential surfaces for a symmetric *syn*- and *anti*-attack of **1** to **11** by means of the EH method yields the energy-difference map shown in Fig. 6. This map shows that the *anti* attack is favoured for all distances. An analysis of the molecular orbitals for the *syn* addition between **1** and **11** indicates that the dominant interaction is a destabilizing 4-center-4-electron-repulsion between the π orbital of the ethylene bridge and the n+ linear combination of the n-orbitals at the nitrogens of **1** (Fig. 7).

The difference between the results for the cycloadditions **7** + **1** and **11** + **1** can be ascribed to the different energy values for the π levels and to the different AO coefficients in the wave functions. In **7** π_{CO}^*

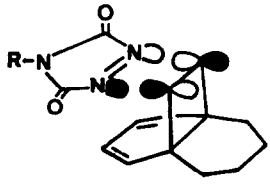

Fig. 5. Schematic drawing of the π^* orbital of the ethylene bridge of **5** and the n_ combination of **1**.

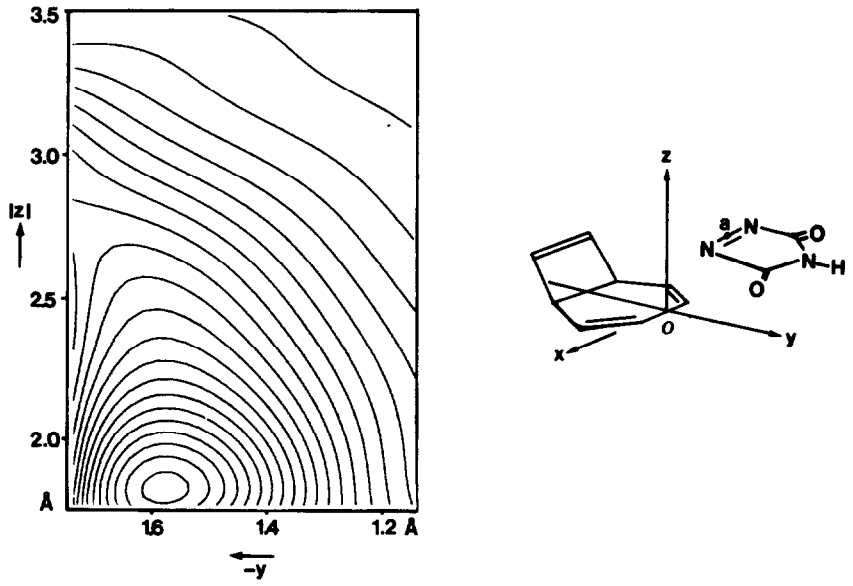

Fig. 6. Analogous contour diagram to that shown in Fig. 3 for the reaction of 1 with 11.

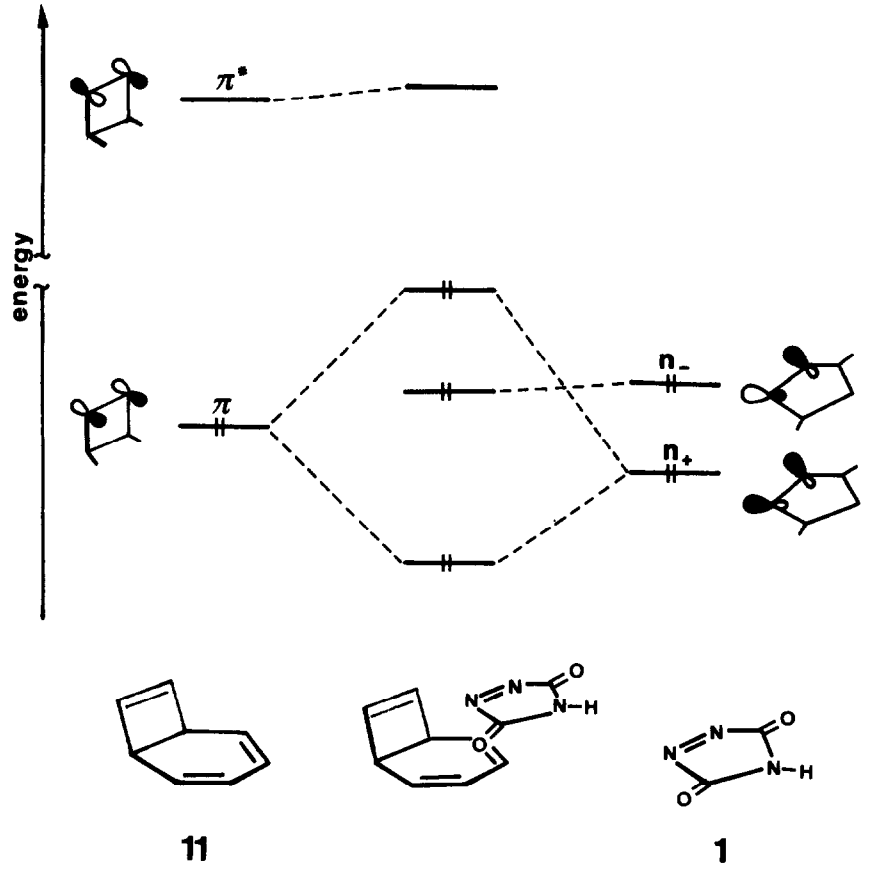

Fig. 7. Qualitative interaction diagram between the ethylene part of 11 and the lone-pairs on the nitrogen atoms of 1.

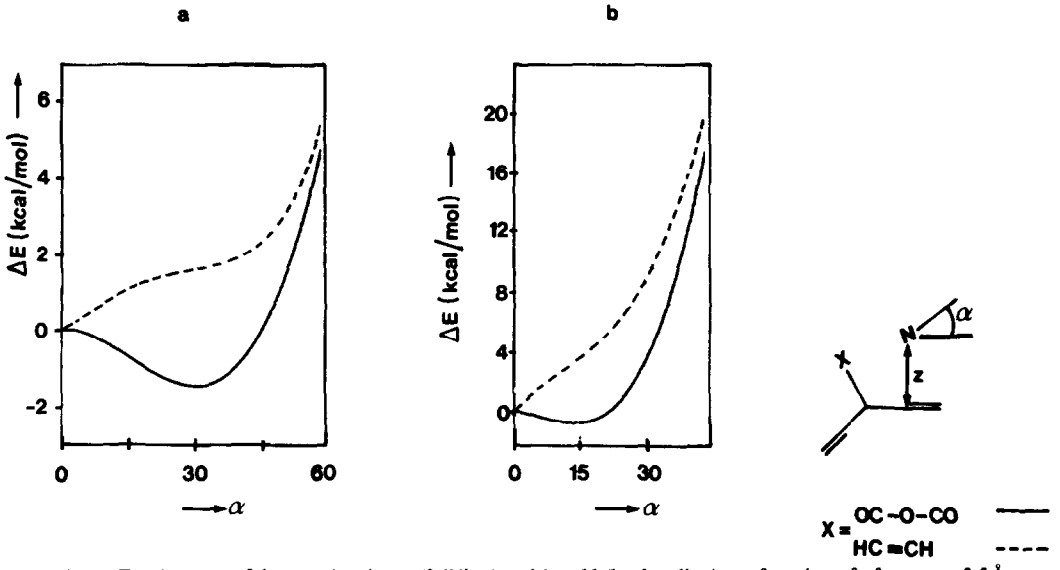

Fig. 8. Total energy of the reaction **1** + **7** (full line) and **1** + **11** (broken line) as a function of α for z = +3.5 Å (**a**) and z = +3.0 Å (**b**) at y = −1.16 Å. The zero point of energy has been chosen for α = 0°.

has the largest amplitude at the carbon centers while the corresponding π_{CO} is more localised at the O atoms. From this only the interaction between π^* and n_- leads to a considerable overlap of both fragments. On the other hand, the AO coefficients of π and π^* of the ethylenic double bond in **11** are the same and thus the (identical) overlap integrals with the corresponding n_+ and n_- combination of **1** results. For **1** a net destabilisation results since π and n_+ are closer in energy than π^* and n_-. A comparison between calculated transition state geometries for a Diels–Alder reaction with the results of the energy-difference map (Fig. 6) shows that *syn* attack leads to a destabilisation of 5 to 13 kcal/mol.

Our model calculations on the Diels–Alder reaction between **1** and **11** suggest that a reaction between **1** and an ethylene bridged diene in which the *anti*-attack is hindered might occur via a two step mechanism. If the *anti*-attack is unfavoured for steric reasons then a *syn* attack of **1** might prefer a transition state of lower symmetry than C_s. As a corollary in the consideration of a secondary orbital effect between the hetero-ring in systems like **2** or **3** it follows that the attack of **1** for +z distances (Fig. 8) about 3 Å should occur perpendiculary to that ring and not parallel to the diene system. To check this we varied the angle α for distances between 4 Å and 2 Å for y = −1.16 Å. The results for z = 3.5 Å are shown in Fig. 8(a) for the addition of **1** to **7** and to **11**. In Fig. 8b the results for z = 3.0 Å are displayed. For the reaction of **1** and **7** we find a minimum for the total energy for α = 35° (z = 3.5 Å) and α = 17° for z = 3.0 Å. At larger distances (4 Å) no minimum is encountered and at smaller z distances (2 Å) the interaction with the diene system dominates. In case of **1** and **11** no minimum is encountered for all distances described above (Fig. 8).

Due to the nonorthogonality of the π system in the propellanes **2**, **3** and **6** $\sigma|\pi$ interaction takes place. In Fig. 9 we show the relevant precanonical σ orbitals (9a) and π orbitals (9b) for **2**, **3** and **6** obtained from an analysis of the Extended Hückel wave functions based on the procedure given by Heilbronner and Schmelzer.[17]

The interaction of the precanonical orbitals $a_2'(\pi)$ and $b_2'(\pi)$ with $a_2'(\sigma)$ and $b_2'(\sigma)$, respectively, can be represented as giving rise to a rotation of the $p\pi$ lobes participating in the resulting canonical orbitals. In case of $a_2(\pi)$ (Fig. 9(c)) the terminal lobes of each butadiene unit are rotated away from the bridge, while

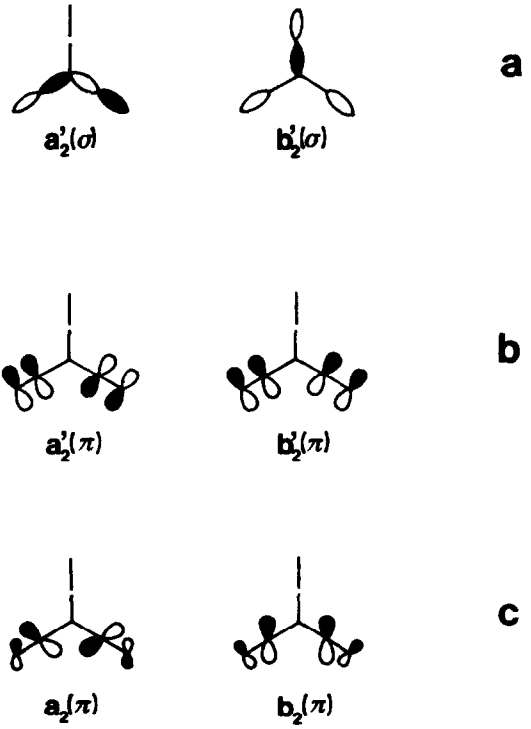

Fig. 9. Precanonical orbitals $a_2'(\sigma)$, $b_2'(\sigma)$ (**a**), $a_2'(\pi)$ $b_2(\pi)$ (**b**) of **2**, **3** and **6** viewed from the bridge-head. Resulting canonical π orbitals (**c**).

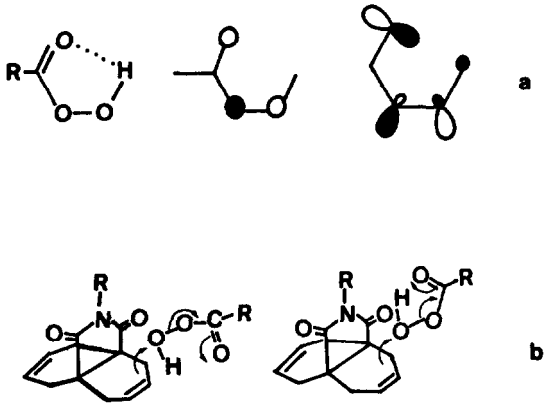

Fig. 10. Schematic drawing of the two highest occupied molecular orbitals of an alkylperacid (**a**) together with two possible geometries for a transition state (**b**).

for $b_2(\pi)$ (Fig. 9(c)) a rotation in the opposite sense is observed. As a result, frontier orbital interaction with $a_2(\pi)$ and $b_2(\pi)$ favours attack from "above" and "below", respectively. In a first order consideration the effects of both types of rotation in the diene system seem to cancel each other.

In every case the effects of $\sigma|\pi$ interaction are overruled bv secondary orbital interaction. This is responsible for a preorientation of the dienophile attack at larger distances while the influence of orbital rotation is limited to the transition state.

Another example which can be explained by invoking secondary orbital effects is the high selectivity of the peracid oxidation of **12** to the *syn* product.[18] In Fig. 10 the two highest occupied MO's of an alkylperacid are shown together with possible geometries of assumed transition states. For both cases π^*_{CO} interacts in a bonding fashion with the n_ combination of the –OOH group or with the π-orbital.

Also the observation that **12** and **13** prefer the *exo-exo* conformation in the solid state[19,20] while most other 3,8-dienes exist in the *endo-endo* or *endo-exo* conformation[21,22] can be rationalized using secondary orbital effects. In these two examples an intramolecular secondary orbital interaction between the π-orbitals of the cyclohexene units and the π^* contribution of the carbonyl bridge may stabilize the *exo–exo* isomer as indicated schematically in Fig. 11.

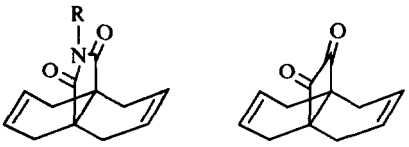

12 **13**

exo-exo *endo-endo* *exo-endo*

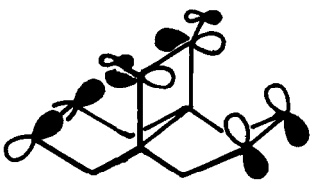

Fig. 11. Spatial interaction between the π_- combination and a low lying empty orbital of **13** in the *exo–exo* conformation.

Cycloaddition reactions of propellanes with a SO_2 *and* SO *bridge*

In the propellanes **14** and **15** preferential *syn* addition of **1** is observed.[3]

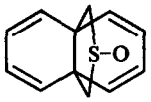

14

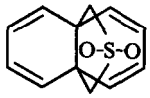

15

We did not succeed in rationalising this behaviour by considering the frontier orbitals as in the foregoing paragraph and it is necessary to go beyond this approach. Therefore we made use of the perturbational model for the treatment of reactions developed by Hudson and Klopman.[23–25] Within this approximation the total gained interaction energy ΔE is divided into two parts called I and II as follows:

$$\Delta E = \sum_{A<B}\sum \frac{q_A \cdot q_B \cdot e^2}{R_{AB}} + \left(\sum_i^{occ}\sum_j^{unocc} - \sum_i^{unocc}\sum_j^{occ}\right)\delta\varepsilon_{ij}$$

I II

q_A = net charge at center A

$$-\delta\varepsilon_{ij} = \frac{C_{iA}^2 \cdot C_{jB}^2}{\varepsilon_i - \varepsilon_i}\beta_{AB}^2$$

R_{AB} = distance between centers A and B
C_{iA} = LCAO coefficient of orbital i at center A
ε_i = orbital energy of MO i
β_{AB} = resonance integral between center A and B

In this equation the Coulomb-term I takes into account the electrostatic interaction between the centers A and B, while the covalent-term II characterises the bond formation between the corresponding centers or fragments. The first term dominates if there is a large energy gap between the niveaus of the interacting fragments and if both centers carry a considerable net charge. The second term dominates (i.e. frontier orbital control results) if the energy gap is small and the fragments overlap significantly. In Fig. 12 the two limiting cases of charge control (I) and frontier orbital control (II) are shown schematically.

For secondary interactions in case of a reaction between **1** and **14** or **15** clearly charge control is

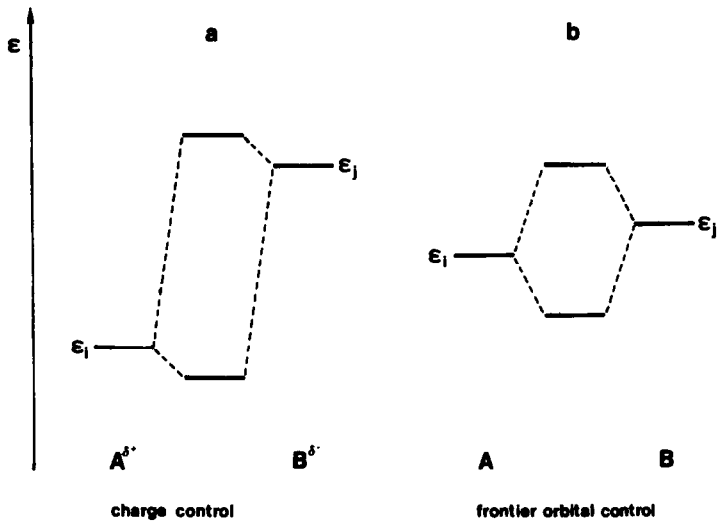

Fig. 12. MO Scheme for a reaction in which (a) the reactants A and B carry a considerable net charge with a large HOMO–LUMO gap and (b) without considerable net charge and small HOMO–LUMO gap.

important since both compounds possess highly polar groups in the bridge.[3] Furthermore there is a large energy gap between the highest occupied molecular orbitals of **1** and the unoccupied levels of the SO_2 or SO group in **14** and **15**, respectively. To understand the directing effect operating in case of **14** or **15** it is necessary to have a physical term which rationalizes pictorially the electrostatic interaction between the reacting species. A quantum chemical expectation value which meets this challenge is the electrostatic potential (EP) of a molecule exerted on a test charge. In line with the definition of the EP a positive point charge acts as a probe to test the potential around the molecule. We have calculated the EP in a modified central field monopole approximation[26] according to eqn (2a).

$$EP(P) = \sum_A \frac{Z_A}{R_{AP}} - \sum_{ij} P_{ij} \int \frac{\psi_i \psi_j}{r_P} d\tau \qquad (2)$$

$$EP(P) \approx \sum_A \frac{Q_A}{R_{AP}} \qquad (2a)$$

EP(P) = electrostatic potential acting on a positive point charge at P
Z_A = core charge
Q_A = net charge
P_{ij} = first order density matrix.

For a qualitative discussion approximation (2a) is sufficient[27] and the calculations are less time consuming than by considering eqn (2).[28]

Recently the electrostatic potential has been used to rationalise electrophilic protonations.[27,29,30] In an extension of this application we have calculated the EP in **1**, **14** and **15** using the EH method[31] and compared the obtained EP maps to obtain information about attractive regions for Coulomb interaction.

Inspection of Fig. 13 displays that the preferred *syn* attack in case of **14** can be rationalised as due to a stabilising Coulomb attraction between the strongly electron deficient S atom in the SO_2 group and the electron-rich N_2 group in **1**. Besides the interaction just discussed there is still another electrostatic interaction present between the area of high electron density around the oxygen centers of the SO_2 fragment and the charge-deficient region above and below the π-plane of **1**.

This interaction is sketched below.

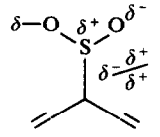

In Fig. 13 we also have plotted the EP of **15**. The resulting potential shows areas of Coulombic attraction on the oxygen side and on the unsubstituted side of the sulfur.

According to our model calculations and the discussion given above we expect the attack of the first dienophile at the "unsubstituted" *syn* side of **14**. This position has less steric interaction than the *syn*-oxygen side and shows a highly attractive potential due to polarisation of the electron density. The crucial Coulomb interaction determining the stereochemistry of the Diels–Alder reaction between **1** and **14** is the interaction between the positively charged S atom and the N-lone-pairs of **1**. More sophisticated *ab initio* calculations on related systems[32] show that in fragments like SO there is no long range effect from the lone-pair but only a positive potential effect as a result of the weak screening of the S core. The experimental work justifies this prediction only in part. The sulfoxide **14** gives one monoadduct **16** produced by *syn* attack and two bis-adducts **17** and **18** which result from the isolated *anti*-monoadduct and the unisolated ones.

For the sulfoxides of different configurations corresponding to structure **19**, both mono-adducts isolated were shown to be the *syn*-products **20** and **21**.[7]

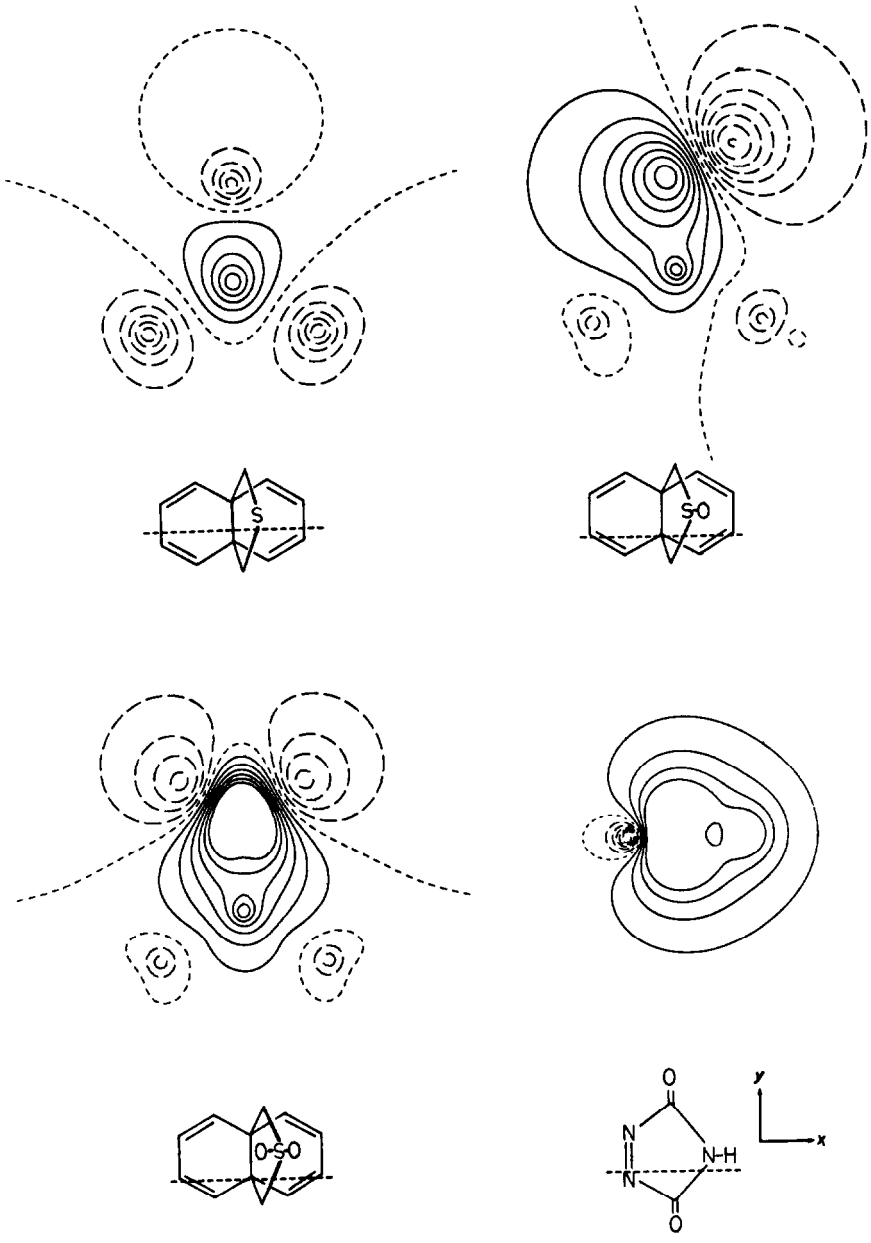

Fig. 13. Contour diagrams of the calculated electrostatic potentials **1**, **6** (X=S), **14** and **15**. The maps are drawn in the plane parallel to the z, x-plane indicated by the dashed line in the formulae. The interval between the contours is 15 kcal/mol in the case of **6** (X=S) and 30 kcal/mol in the case of **1**, **14** and **15**. Positive potentials are indicated with full lines, negative potentials with broken lines. Nodes are indicated by short dashes.

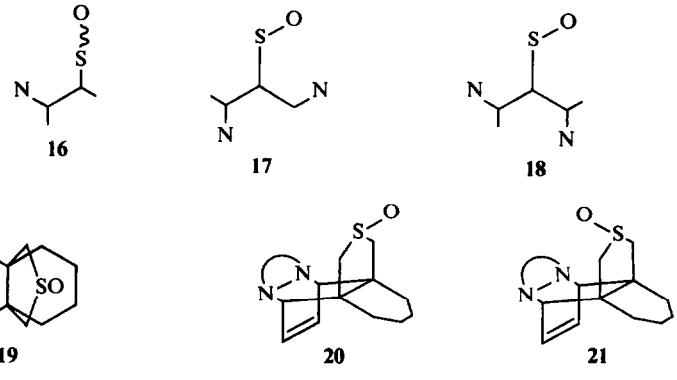

Acknowledgement—These investigations were initiated and stimulated by Prof. D. Ginsburg. For financial support we thank the Deutsche Forschungsgemeinschaft and the Fonds der Chemischen Industrie. We are grateful to the Deutscher Akademischer Austauschdienst for making possible the visit of Prof. Ginsburg in Heidelberg in Summer 1979.

REFERENCES

[1]D. Ginsburg, *Propellanes, Structure and Reactions.* Verlag Chemie, Weinheim (1975).
[2]D. Ginsburg, *Accounts Chem. Res.* **7,** 286 (1974).
[3]R. Gleiter and D. Ginsburg, *Pure Appl. Chem.* **51,** 1301 (1979) and Refs. therein.
[4]P. Ashkenazi, D. Ginsburg, G. Scharf and B. Fuchs, *Tetrahedron* **33,** 1345 (1977).
[5]E. Heilbronner and H. Bock, *Das HMO Modell und seine Anwendung. Verlag Chemie, Weinheim* (1970); M. J. S. Dewar and R. C. Dougherty, *The PMO Theory of Organic Chemistry.* Plenum Press, New York (1975).
[6]J. Kalo, D. Ginsburg and E. Vogel, *Tetrahedron* **33,** 1177 (1977).
[7]J. Kalo, E. Vogel and D. Ginsburg, *Ibid.* **33,** 1183 (1977).
[8]R. Hoffmann, *J. Chem. Phys.* **39,** 1397 (1963); R. Hoffmann and W. N. Lipscomb, *Ibid.* **36,** 2179, 3489 (1962); *Ibid.* **37,** 2872 (1962).
[9]M. J. S. Dewar, A. C. Griffin and S. Kirschner, *J. Am. Chem. Soc.* **96,** 6225 (1974).
[10]L. A. Burke, G. Leroy and M. Sana, *Theoret. Chim. Acta* **40,** 313 (1975).
[11]R. E. Townsend, G. Ramunni, G. Segal, W.-J. Hehre and L. Salem, *J. Am. Chem. Soc.* **98,** 2190 (1976).
[12]Critical analysis of the results discussed in Ref. 9 to 11 by P. Caramella, K. N. Houk and L. N. Domelsmith, *Ibid.* **99,** 4511 (1977).
[13]J. E. Baldwin and R. H. Fleming, *Topics in Current Chemistry* **15,** 281 (1970).
[14]K. N. Houk and L. L. Munchhausen, *J. Am. Chem. Soc.* **98,** 937 (1976).
[15]D. Rowley and H. Steiner, *Disc. Faraday Soc.* **10,** 198 (1951).
[16]J. Kalo, J. M. Photis, L. A. Paquette, E. Vogel and D. Ginsburg, *Tetrahedron* **32,** 1013 (1976).
[17]E. Heilbronner and A. Schmelzer, *Helv. Chim. Acta* **58,** 936 (1975).
[18]W. J. W. Mayer, I. Oren and D. Ginsburg, *Tetrahedron* **33,** 1345 (1977).
[19]M. Kaftory and J. D. Dunitz, *Acta Cryst.* B **32,** 617 (1976).
[20]S. C. Neely, R. Fink, D. van der Helm and J. J. Bloomfield, *J. Am. Chem. Soc.* **93,** 4903 (1971).
[21]C. Amith, M. Hackmeyer and D. Ginsburg, *Tetrahedron* **32,** 1015 (1976).
[22]M. C. Böhm and R. Gleiter, *Ibid.* **35,** 675 (1979).
[23]G. Klopman, *J. Am. Chem. Soc.* **90,** 223 (1967).
[24]G. Klopman and R. F. Hudson, *Theor. Chim. Acta* **8,** 165 (1967).
[25]R. F. Hudson and G. Klopman, *Tetrahedron Letters* 1103 (1967).
[26]E. U. Condon and G. H. Shortley, *The Theory of Atomic Spectra,* Cambridge University Press (1970).
[27]J. Almlöf, E. Haselbach, F. Jachimowicz and J. Kowalewski, *Helv. Chim. Acta* **58,** 2403 (1975).
[28]C. Giessner-Prettre and A. Pullman, *Theor. Chim. Acta* **25,** 83 (1972).
[29]E. Scrocco and J. Tomasi, *Topics in Current Chemistry* **42,** 95 (1973).
[30]J. Almlöf, A. Hendriksson-Enflo, J. Kowalewski and M. Sundbohm, *Chem. Phys. Lett.* **21,** 560 (1973).
[31]Although the EH method exaggerates charge separation (F. Driessler and W. Kutzelnigg, *Theor. Chim. Acta* **43,** 307 (1977)) it should be sufficient for our qualitative discussion.
[32]R. Bonaccorsi, A. Pullman, E. Scrocco and J. Tomasi, *Chem. Phys. Letters* **12,** 622 (1972).